Designing Freeform Micro Lens Array With Prescribed Luminous Intensity for LCD Backlight Units

Zhengbo Zhu, Le Yang, and Donglin Ma

***Abstract*—The precise luminous intensity control for liquid crystal display (LCD) backlight units is an important issue that has not been well addressed in current research. A proper luminous intensity distribution can significantly enhance the viewing experience. In this paper, we propose a method for designing a freeform micro lens array that is capable of producing a prescribed luminous intensity distribution for direct-lit LED backlight module. As the luminous intensity distribution is usually need to be constrained within a quadrilateral pyramid region, a special coordinate system is developed by scanning two semicircles containing light rays along the X axis and Y axis to provide a flexible model for luminous intensity tailoring. Further, we convert the luminous intensity design problem to a specific illuminance problem by using a lossless energy conversion strategy. Then, an integrable ray mapping between the source domain and the target domain is established to implement the freeform optics design to regulate the converted illuminance distribution. The effectiveness of the proposed method is verified via various design examples including on-axis configuration and axis-off configuration, the influence of the LED size on the optical performance is also analyzed.**

***Index Terms*—Backlight system, freeform optics design, LED, micro lens array.**

I. Introduction

LEDs (light-emitting diodes) offer several advantages over the traditional light sources, which have made LED backlighting a popular choice for liquid-crystal display (LCD) applications, including consumer electronics, automotive displays, and medical displays, among others. The direct-lit LED backlight unit (BLU) is a crucial component of large-area LCD and high-brightness LCDs displays. It aims to produce high-quality lighting effects by evenly placing a series of LEDs behind the LCD panel. The image quality of the LCD significantly relies on the illumination quality of the direct-lit LED BLU.

Extensive research has been done on designing direct-lit LED BLU for LCD applications [1], [2], [3], [7]. For instance, Ding et al. designed compact lenses to tailor the light from extended LED sources, the thin and high-quality direct-lit LED backlight systems have been realized [1]. Kikuchi et al. optimized the size and arrangement of reflective dots to obtain a higher uniform luminance distribution and a broader light distribution with a small number of mini-LEDs [3]. Yoon et al. designed a semi-partitioned light guide plate patterned with inverse-trapezoidal microstructures, which achieved uniformity in both local and global luminance distributions, as well as a local dimming ability [6]. These works are mostly involved in pursuing more uniform illuminance distribution for LCDs, reducing the thickness of the BLU while maintaining high brightness, realizing the local dimming capability, and so on.

However, for some special LCD applications including anti-peeping screens and head up displays, it is crucial for the LCDs to be visible only within a certain angular space and to evenly distribute the luminous intensity of the screen across this range of viewing angles. Taking the LCD in head up display as an example, if the luminous intensity of the BLU is Gaussian, stray light will be inevitably generated in the optical system, and the contrast of the picture observed by the human will be reduced, thus leading to visual fatigue of the driver and endangering driving safety [8], [9]. For these special applications, the precise luminous intensity control of the direct-lit LED BLU is extremely important. To achieve the prescribed luminous intensity distribution, brightness enhancement films and privacy filters are commonly adopted at the expense of the overall brightness of the LCD, and stray light is also hard to be avoided [10], [11], [12].

In previous work [13], [14], we have explored the freeform illumination optics design method to achieve prescribed illuminance distribution, which proves the strong illuminance control ability of freeform optics. Here, we develop a method for designing a freeform micro lens array (MLA) that is utilized in a direct-lit LED backlight module and capable of producing a prescribed luminous intensity distribution. A reference

Manuscript received 10 April 2023; accepted 14 April 2023. Date of publication 5 May 2023; date of current version 19 May 2023. This work was supported in part by the National Natural Science Foundation of China under Grants 12274156 and 62205116, in part by the Key Research and Development Program of Hubei Province under Grant 2020BAB121, in part by The Postdoctoral Innovative Research Project of Hubei Province in 2022, in part by China Postdoctoral Science Foundation under Grant 2022M711244, and in part by the Science, Technology and Innovation Commission of Shenzhen Municipality under Grants JCYJ20190809100811375 and JCYJ20210324115812035. *(Corresponding author: Le Yang.)*

Zhengbo Zhu is with the School of Optical and Electronic Information and Wuhan National Laboratory for Optoelectronics, Huazhong University of Science and Technology, Wuhan 430074, China (e-mail: zhuzb@hust.edu.cn).

Donglin Ma is with the School of Optical and Electronic Information and Wuhan National Laboratory for Optoelectronics, Huazhong University of Science and Technology, Wuhan 430074, China, and also with the MOE Key Laboratory of Fundamental Physical Quantities Measurement and Hubei Key Laboratory of Gravitation and Quantum Physics, PGMF and School of Physics, Huazhong University of Science and Technology, Wuhan 430074, China (e-mail: madonglin@hust.edu.cn).

Le Yang is with the Department of Emergency Medicine, Department of Critical Care Medicine, Tongji Hospital, Tongji Medical College, Huazhong University of Science and Technology, Wuhan 430030, China (e-mail: leyang666@163.com).

Digital Object Identifier 10.1109/JPHOT.2023.3267888

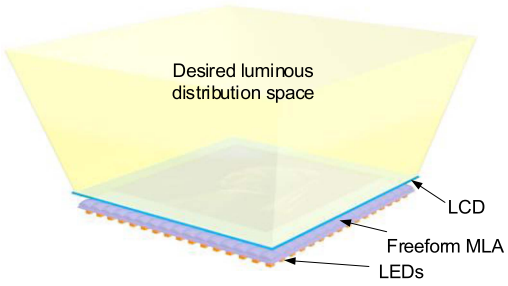

Fig. 1. Geometrical layout of the freeform MLA based backlight system for LCD.

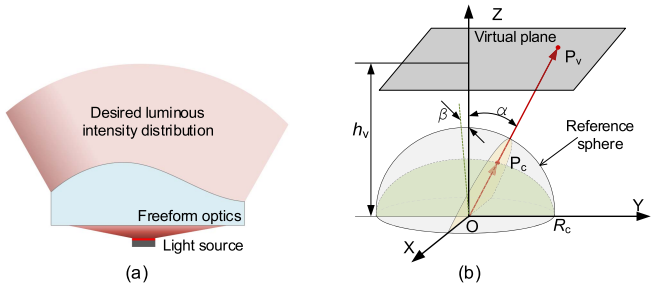

Fig. 2. (a) The sketch of the luminous intensity control; (b) the geometrical design layout.

spherical surface and a virtual plane are employed in the design process, and a light conversion strategy is adopted to convert the luminous intensity distribution problem to an illuminance distribution problem via a numerical transformation. Then, we design a freeform MLA to achieve the converted illuminance distribution on the virtual plane, thereby, the required luminous intensity distribution can be achieved. The whole design process that combines the problem statement, the light conversion strategy and the ray mapping method is detailed in Section II. In Section III, we provided several challenging examples to prove the feasibility of the proposed method, and elaborate analyses of the designs are also made in this section before we conclude our work in Section IV.

II. Design Methodology

The conceptual configuration of the freeform MLA based backlight system for LCD with specific luminous intensity distribution is presented in Fig. 1. A series of LED light sources with identical parameters are evenly arranged, and the freeform MLA is positioned between the LCD panel and the LEDs. Each LED is precisely aligned with the center of its corresponding sub-lens, which has the same shape and size. The freeform MLA is used to controls the light beam emitted by the LEDs, with the objective of achieving a specific luminous intensity distribution within a specified angle range, while maintaining a uniform illuminance distribution on the LCD panel. This unique backlight unit is similar to the directional backlight which is typically used in 3D displays [15], [16], but has a simpler structure and non-adjustable directivity.

A. Light Conversion Strategy

At present, most of the published research on freeform illumination optics design is primarily involved in achieving a specific illuminance distribution on the pre-determined target [13], [14], [17], [18], [19], [20], [21]. If the relation between illuminance distribution and intensity distribution can be established by a mathematical model, the problem of intensity distribution regulation might be transformed into an illuminance control problem. In this section, we establish this potential mathematical model to convert the problem of generating the specific intensity distribution of LCD panel into designing freeform optics for the corresponding illuminance distribution problem.

Fig. 2(a) depicts the sketch of the luminous intensity control. A light source is located at the origin of the global coordinate system, which emits light in the up-half space. The freeform lens to be designed redistributes the incoming rays from the light source to achieve a prescribed intensity distribution. The regulation of rotationally symmetric luminous intensity distribution has been well solved [22]. However, for some special illumination systems, luminous intensity distributions with non-rotationally symmetric characteristic are commonly required. For instance, the luminous intensity is required to be distributed within a certain range of angles up and down, as well as a certain range of angles left and right, that is to form a quadrilateral pyramid like spatial luminous intensity distribution. This leads us to establish a special coordinates system (α, β) for tackling the light regulation problem of LCD panel, which will be described in detail below.

Luminous intensity refers to the light flux within a unit solid angle in a given direction of a light source [23]. Assuming a reference spherical surface exists with its center located at the light source, the illuminance value generated by the light beam at the point of intersection with the spherical surface is proportional to the intensity value corresponding to the angle of the light beam.

Based on the above analysis of the relationship between luminous intensity and illuminance, a reference semi-spherical surface is introduced with its center located at the origin, as shown in Fig. 2(b). The prescribed luminous intensity distribution on the spherical surface is defined in terms of illuminance information, thus converting the luminous intensity design problem to an illuminance control problem on the spherical surface. However, a precise light control on a 3D target is more challenging than that of the conventional plane targets. Inspired by our previous research [24], we further employ a virtual plane that is perpendicular to the optical axis. The illuminance distribution on the reference spherical surface is then further converted to the virtual plane, thus transforming the initial luminous intensity problem into an illuminance distribution problem.

The height of the virtual plane is preset as h_v, and the radius of the reference sphere is R_c. In analyzing the distribution of luminous intensity in a far-field configuration, the sizes of the optical element and light source can be ignored compared with the whole illumination system. We directly trace rays from the origin to the reference hemispherical surface and virtual plane in sequence, the information of the intersection points P_c (x_c,

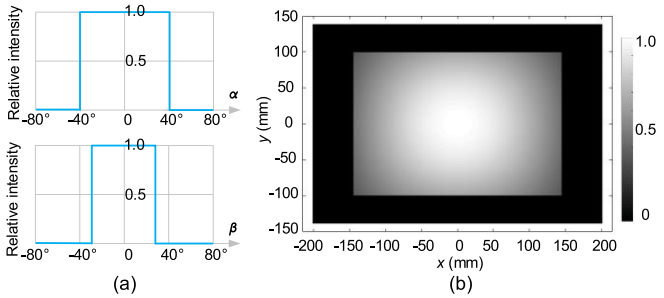

Fig. 3. (a) The prescribed luminous intensity distribution in X direction (up) and Y direction (down), (b) the corresponding illuminance distribution on the virtual plane at z = 200 mm.

y_c, z_c) and P$_v$ (x_v, y_v, h_v) can be calculated as:

$$\begin{cases} x_c = R_c \tan\alpha \Big/ \sqrt{(\tan\alpha)^2 + (\tan\beta)^2 + 1} \\ y_c = R_c \tan\beta \Big/ \sqrt{(\tan\alpha)^2 + (\tan\beta)^2 + 1} \\ z_c = R_c \sqrt{1 - x_c^2 + y_c^2} \end{cases}, \quad (1)$$

$$\begin{cases} x_v = (h_v - z_c)\, x_c / z_c + x_c \\ y_v = (h_v - z_c)\, y_c / z_c + y_c \end{cases}, \quad (2)$$

where α is the angle between the X–Z plane and the yellow shaded surface containing light ray OP$_c$ and axis OX, and β represents the angle between the Y–Z plane and the green shaded surface containing light ray OP$_c$ and axis OY, as shown Fig. 2(b). The luminous intensity distribution is denoted as I (α, β). The proposed representation of intensity directly connects the light distribution with the required quadrilateral pyramid region of the LCD panel luminescence, which is more convenient and straightforward compared with the traditional intensity defined on spherical coordinates. The illuminance distribution on the reference spherical surface can now be calculated by a parametric space {α, β}, i.e, E_c (x_c, y_c) = f (α, β). Further, the illuminance distribution E_v (x_v, y_v) on the virtual plane can be deduced with the assumption of a lossless system:

$$E_v(x_v, y_v) = E_c(x_c, y_c) \frac{\partial(x_c, y_c)}{\partial(x_v, y_v)}, \quad (3)$$

where ∂ (g$_1$, g$_1$) / ∂ (a_1, a_2) denotes the Jacobian of vector-value function **g** (g$_1$, g$_1$) to variables (a_1, a_2). So far, the luminous intensity distribution I (α, β) in the three-dimensional space has been successfully converted to the illuminance distribution E_v (x_v, y_v) in the two-dimensional space.

We give a design example to demonstrate the effectiveness of the above light conversion method. In a quadrilateral pyramid like space {(α, β) | |α|≤40°, |β|≤30°}, a uniform luminous intensity distribution is desired as illustrated in Fig. 3(a), the illuminance distribution on the virtual plane with a height of h_v = 200 mm is calculated as shown in Fig. 3(b). It clearly shows that the illuminance distribution on the virtual plane is non-uniform. And the next work in this section is to design a freeform lens to redistribute the light from the LED to form the converted illuminance distribution E_v (x_v, y_v) on the virtual plane, and further verify the optical performance of the corresponding freeform MLA.

B. Ray Mapping Process

In this section, we will design the freeform lens for generating a predetermined illuminance on the virtual plane obtained in the previous section. It should be noted that all the well-developed zero-étendue methods can be used. For our purpose, we will utilize the so-called ray mapping method [24], [25] to complete the design. The ray mapping method is to solve a mapping relation between the source domain and the target domain satisfying the flux conservation and the boundary condition:

$$E_s(x_s, y_s) = E_v(\mathbf{m}(x_s, y_s)) \frac{\partial(m_1, m_2)}{\partial(x_s, y_s)}, (x_s, y_s) \in S,$$
$$\mathbf{m}(\partial S) = \partial V, \quad (4)$$

where E_s and E_v are the illuminances on the source and the virtual plane respectively. The rays from the source with positions (x_s, y_s) are mapped to the virtual plane on positions **m** = (m_1, m_2), and the notation ∂ denotes the boundary of domains. The surface is constructed based on the solved mapping to achieve the precise light control. However, the surface may fail to redirect the light rays to the desired positions. This leads to the most critical problem in ray mapping methods that the resulting normal field **N** of the surface should satisfy the integrability condition **N**· curl (**N**) = 0.

The integrability condition is not straightforward for solving a ray mapping connected with (4). Here, we transform the constraints of normal fields to the output ray bundles. According to the *Theorem of Malus and Duplin* [26]: If a system of rays constituting a normal congruence is subjected to any number of reflections and refractions at the surfaces of successive homogeneous media, the congruence remains normal throughout. The theorem requires the output ray bundle produced by the target map being a normal system which means that there is a family of surfaces normal to the rays (the wavefront). Here, we can transform the integrability condition from the normal field to the output ray bundle in the following condition:

$$\frac{\partial \mathbf{O}}{\partial u} \cdot \frac{\partial \mathbf{r}}{\partial v} - \frac{\partial \mathbf{O}}{\partial v} \cdot \frac{\partial \mathbf{r}}{\partial u} = 0, \quad (5)$$

where **O** and **r** are the direction and the position of the ray bundle respectively which is defined on a parametric coordinate (u, v). (5) is also known as the étendue 2D and the quantity should be zero if the rays belong to a normal congruence [27], [28]. An iterative process should be implemented to obtain the ray mapping that can produce an integrable ray bundle. Assuming that **r** is the points on the freeform surface in one iteration, the direction **O** can be calculated by (**m** - **r**) / | **m** - **r** | where **m** is positions of the current ray mapping on the virtual plane. Substituting **O** into (5), we can obtain the relation of the integrability condition to the ray mapping **m** and the partial derivatives (∂**m**/∂u, ∂**m**/∂v).

Directly solving (4) with constraints (5) is a complex task. Here, we employ a heuristic procedure demonstrated in our previous work [24], [25]. Instead of solving a ray map satisfying

(5), this method traces the rays through the current surface which will lead to a mapping automatically satisfy (5) and corrects the mapping to satisfy (4) with limit variation of its first partial derivative. The method can be regarded as the process to iteratively correct an integrable ray map to approach energy conservation and boundary condition. The detailed method can be found in [24], [25].

III. Design Examples

In this section, some examples are provided to verify the effectiveness of the proposed method. The polymethyl methacrylate (PMMA) with a refractive index of 1.49 is chosen as the material of the freeform MLA, and light sources are LEDs with Lambertian property. The entrance surface of the MLA is chosen as flat for the convenience of manufacturing. LightTools is implemented to conduct optical performance analysis based on Monte-Carlo ray tracing. For all examples, the resolutions of luminous intensity distribution and illuminance distribution on the LCD are set as 60 × 60 and 80 × 80, respectively.

In the first design example, the goal is to generate a uniform luminous intensity within the angle space of $\{(\alpha, \beta)| |\alpha| \leq 40°, |\beta| \leq 35°\}$. This design will detail the whole design process of the above method. Firstly, we convert the required luminous intensity into the illuminance distribution on the reference spherical surface using (1), and the result is given in Fig. 4. (a), which shows a uniform illuminance distribution. Secondly, we introduce a virtual plane perpendicular to the Z axis at z = 200 mm. The distance between the virtual plane and the light source is insignificant since the relative illuminance distribution generated on different parallel planes is consistent. By using (2) and (3), the calculated illuminance distribution on the virtual plane is presented in Fig. 4(b), which shows a non-uniform illuminance distribution with a rectangular shape.

Now, we will proceed to design a single freeform lens to generate the converted illuminance distribution on the virtual plane. The distance between the LED and the incident surface of the MLA is fixed at 0.5 mm. The obtained ray mapping **m** between the source map and the target map via (4) and (5) is presented in Fig. 4(c), where 201 × 201 grids are interpolated into 31 × 31 grids for better visualization. The arrow in the figure indicates that the ray mapping maps the energy within the grid of the source domain to the corresponding grid in the target domain in sequence. Next, we employ the method introduced in Ref. [29] to calculate the point cloud of the freeform surface and use 3D modeling software to construct a solid model of the freeform lens.

The obtained single freeform lens model is depicted in Fig. 4(d), the size of the lens is 4.10 mm × 3.96 mm × 1.72 mm (length, width and height). A point-like LED source (LED chip: 0.05 mm × 0.05 mm) is assumed, whose size is negligible compared with the freeform lens. The Monte Carlo ray tracing method is adopted here to verify the light control capability of the obtained freeform lens. Then, we trace 200 million rays, and the simulated luminous intensity distribution is shown in Fig. 4(e). The cutoff line of the angular distribution is clear, and

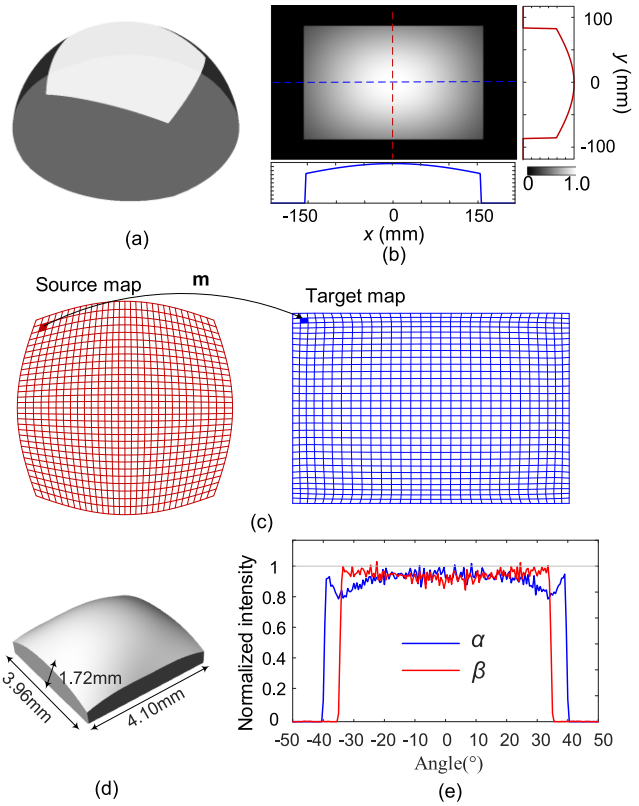

Fig. 4. Design results of the single freeform lens: (a) the illuminance distribution on the reference spherical surface; (b) the converted illuminance distribution on the virtual plane at z = 200 mm; (c) the ray mapping between the source domain and the target domain; (d) the single freeform lens model and (e) the simulated luminous intensity distribution along X axis (blue line) and Y axis (red line).

the range of the luminous intensity distribution is consistent with the desired value, which demonstrates a well light control.

Further, the freeform lenses are arranged to form a micro-lens array (MLA) to assess the light control ability of a direct-lit backlight unit (BLU) for LCDs. As an example, a direct-lit BLU with 11 × 11 lighting modules is presented, as shown in Fig. 5(a).

Initially, a point-like source is still used to verify the optical performance, and the normalized luminous intensity distribution is displayed in Fig. 5(b). It is evident that the luminous intensity regulation capability of the MLA is consistent with that of the single freeform lens (in comparison with Fig. 4(e)). To analyze the uniformity of the illuminance distribution on the LCD, we position an illuminance receiver at z = 6 mm and recorded the illuminance distribution above it. The resulting normalized illuminance distribution is presented in Fig. 5(c), illustrating a uniform illuminance distribution. As a rule of thumb, we use the root mean square (RMS) as the quantitative index to evaluate the uniformity of the illuminance distribution [1]. A smaller RMS value means a more uniform illuminance distribution. The range of 36 mm × 36 mm on the LCD is chosen as the effective lighting area, as plotted by the black dotted border in Fig. 5(c), and the RMS value in this area is found to be 0.0516. To obtain a uniform illuminance on the LCD, it is necessary to adjust the distance between the adjacent LEDs or the distance between

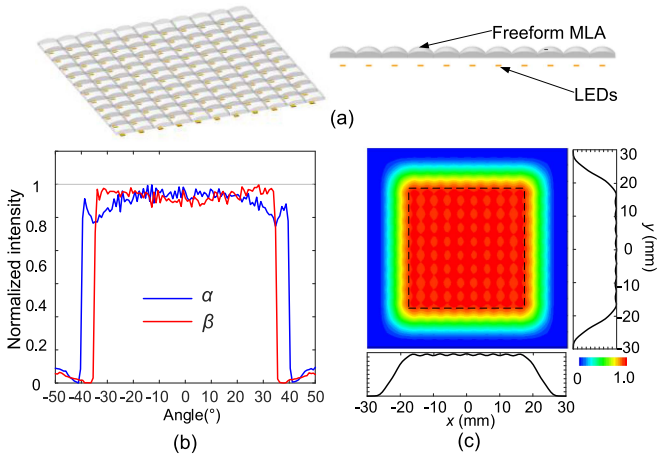

Fig. 5. Design results of the freeform MLA: (a) the diagram of freeform MLA and LEDs; (b) the simulated luminous intensity distribution along X axis (blue line) and Y axis (red line); (c) the normalized illuminance distribution on LCD which is located at z = 6 mm, the black dotted box is the effective lighting area.

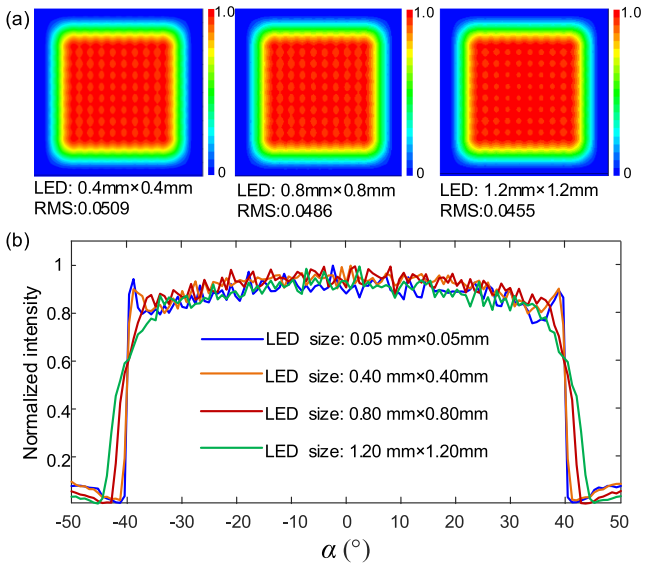

Fig. 6. Optical performances of the designed MLA for different sizes of LED: (a) Illuminance distributions and (b)luminous intensity distributions.

the LED and the LCD, particularly when aiming for a narrower angle of luminous intensity distribution. Specifically, shortening the spacing between adjacent LEDs or increasing the distance between the LED and the LCD would be required.

We investigate the influence of LED size on the light control performance of the designed MLA. The LEDs are varied in size, specifically set as 0.4 mm × 0.4 mm, 0.8 mm × 0.8 mm, and 1.2 mm × 1.2 mm, respectively. We perform a Monte Carlo ray tracing simulation for each configuration, and the resulting illuminance distributions are presented in Fig. 6(a). The RMS values of the illuminance inside the effective lighting area are found to be 0.0509, 0.0486, and 0.0455, respectively. These results suggest that the LED size has minimal effect on the illuminance uniformity on the LCD panel. Fig. 6(b) provides the luminous intensity distributions for different LED sizes. To emphasize the

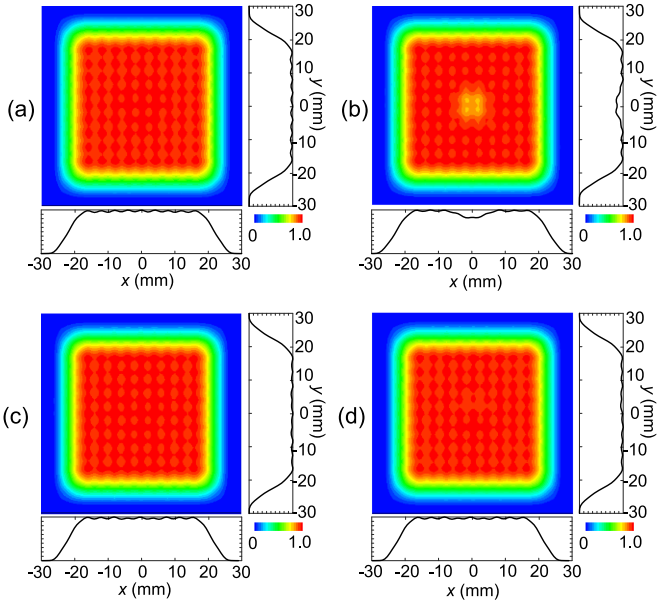

Fig. 7. Illuminance distributions on LCD when the position of the center LED is changed: LED is (a) 0.2 mm closer and (b) 0.2 mm farther to the MLA; (c) LED is moved a distance of 0.2 mm in +Y-axis direction, and (d) LED is s rotated 8° about the Y-axis.

differences more clearly, only the intensity distributions along the X-axis are depicted. The luminous intensity for the point-like LED source is also included for comparison. From this figure we observe that as the LED size increases, the boundary of the luminous intensity distribution becomes more diffuse, resulting in a smoother cutoff line around ±40°. The primary reason for this phenomenon is that as the size of the LED increases, the large angle light rays emanating from the edge of the LED enter the adjacent sub-lens, causing the direction of light propagation to be out of control. However, due to the Lambertian radiation property of the LEDs, the energy carried by these light rays is relatively weak, resulting in insignificant effects on the overall luminous intensity distribution, provided the LED size is not too large.

As installation errors are inevitable in practical engineering, we analyze the effects of installation errors on the optical performance of the designed MLA, specifically focusing on rotational deviation, horizontal deviation, and vertical deviation of the LEDs. For instance, we select LEDs of size 0.8 mm × 0.8 mm and conduct a tolerance analysis on the center LED. Only the change in illuminance distribution is considered, as the position of a single LED has a negligible effect on the overall luminous intensity distribution. Fig. 7(a) and (b) show the simulated results when the center LED source is moved 0.2 mm closer and farther from the MLA, respectively. Fig. 7(c) illustrates the simulated result when the center LED source is moved a distance of 0.2 mm in the +Y-axis direction, while Fig. 7(d) shows the result when the center LED is rotated 8° about the Y-axis. These results indicate that an increase in the distance between the LED and MLA leads to a decrease in illuminance value on the LCD. However, under the condition of small position deviation,

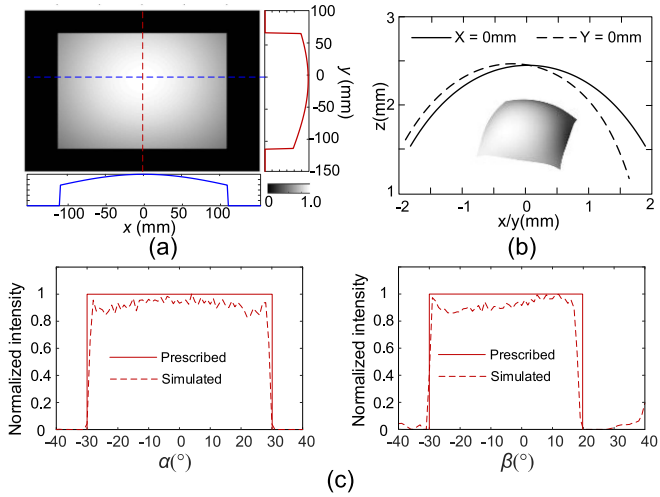

Fig. 8. Design results of the second example for off-axis configuration: (a) The converted illuminance distribution on the virtual plane at z = 200 mm; (b) the lens model and the freeform surface profiles, and (c) the normalized luminous intensity distribution along X axis (left one) and Y axis (right one), the solid line represents the desired intensity and the dashed line denotes the simulated intensity.

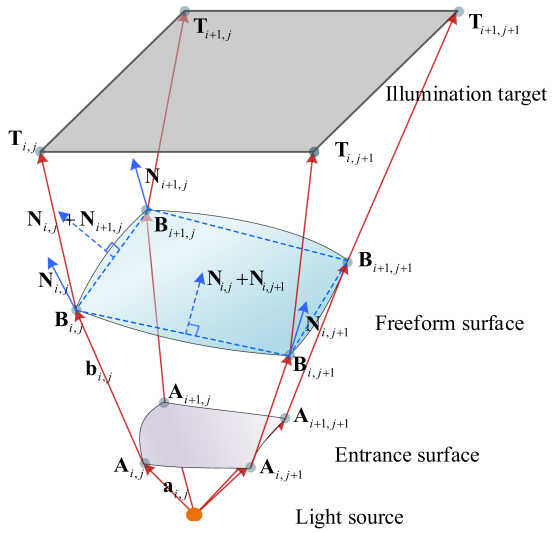

Fig. 9. Sketch of the surface construction from normal vectors.

other forms of LED position offset have little influence on the uniformity of illuminance.

In the second design example, we intend to verify the light control ability of asymmetric intensity distribution of the proposed method, which means that the angle range of the luminous intensity distribution is not symmetrical. This special configuration might have practical applications in super-sized display devices, where the human eye is typically positioned below the center of the screen. For this design, the luminous intensity distribution angle range is set as $\{(\alpha, \beta) \,|\, |\alpha| \leq 30°, -30 \leq \beta \leq 20°\}$, and the required luminous intensity is assumed uniform in this angular space. The normalized illuminance distribution on the virtual plane z = 200 mm is illustrated in Fig. 8(a). This figure illustrates an off-axis light configuration where the center of the illumination region is not on the optical axis. The designed lens model and the corresponding freeform surface profiles are shown in Fig. 8(b), revealing the asymmetry of the designed lens. The simulated luminous intensity distributions along X and Y directions are shown in Fig. 8(c), demonstrating a well agreement with the desired one.

IV. Conclusion

We have developed a novel method for designing freeform optics to achieve prescribed luminous intensity distribution, which can be applied to LCD direct-lit backlight units. For tackling the special luminous intensity distribution of LCD, we build a special coordinate system by scanning two semicircles containing light rays along the X axis and Y axis, which provide a flexible model for tailoring the intensity of LCD panels. By establishing the conversion relationship between luminous intensity distribution and illuminance distribution in three-dimensional space, we have transformed the problem of luminous intensity control into the problem of illuminance regulation. We have also established the ray mapping that can result in integrable surface normal fields between the source domain and the target domain, which is essential for freeform optics design. The effectiveness of the proposed method has been demonstrated through various design examples, including both coaxial and off-axis conditions. Our method is capable of achieving well-controlled luminous intensity distribution for extended LED sources while maintaining uniform illuminance distribution on the LCD panel. The simulation results also show that a compact BLU can be realized by using the proposed freeform optics design method, where the LED size cannot be ignored compared with the freeform lens. Additionally, the proposed method is capable to design MLA for LED displays which directly use a huge number of LEDs to display, as well as design freeform optics for other types of luminous intensity.

Appendix

As shown in Fig. 9, $\mathbf{A}_{i,j}$ denotes the ray intersection on the entrance surface, $\mathbf{B}_{i,j}$ represents ray intersection on the freeform surface. The incident ray sequence $\mathbf{a}_{i,j}$ and the target point sequence $\mathbf{T}_{i,j}$ are determined by the obtained ray mapping illustrated in Fig. 4(c). $\mathbf{b}_{i,j}$ represents the unit ray vector from $\mathbf{A}_{i,j}$ to $\mathbf{B}_{i,j}$. For far field assumption, the outgoing ray sequence can be calculated as $\mathbf{O}_{i,j} = \mathbf{T}_{i,j} / |\, \mathbf{T}_{i,j} \,|$, then the normal vector of the freeform surface can be obtained via Snell's law:

$$\mathbf{N}_{i,j} = \frac{\mathbf{O}_{i,j} - n\mathbf{b}_{i,j}}{|\mathbf{O}_{i,j} - n\mathbf{b}_{i,j}|}, \tag{6}$$

where n represents the refractive index of the lens. Then, the point $\mathbf{B}_{i,j}$ and the normal vector $\mathbf{B}_{i,j}$ can be linked as:

$$\begin{aligned} (\mathbf{B}_{i,j+1} - \mathbf{B}_{i,j}) \cdot (\mathbf{N}_{i,j+1} + \mathbf{N}_{i,j}) = 0, \\ (\mathbf{B}_{i+1,j} - \mathbf{B}_{i,j}) \cdot (\mathbf{N}_{i+1,j} + \mathbf{N}_{i,j}) = 0. \end{aligned} \tag{7}$$

This equation means that the chord connecting the two adjacent points is perpendicular to the average of their normal vectors at these two points. The point $\mathbf{B}_{i,j}$ can be determined

by $a_{i,j}\cdot\mathbf{a}_{i,j+}$ $b_{i,j}\cdot\mathbf{b}_{i,j}$, where $a_{i,j}$ and $b_{i,j}$ represent the distance from light source to point $\mathbf{A}_{i,j}$ and the distance from point $\mathbf{A}_{i,j}$ to point $\mathbf{A}_{i,j}$, espectively:

$$\begin{aligned}\mathbf{B}_{i,j+1} &= a_{i,j+1}\mathbf{a}_{i,j+1} + b_{i,j+1}\mathbf{b}_{i,j+1},\\ \mathbf{B}_{i+1,j} &= a_{i+1,j}\mathbf{a}_{i+1,j} + b_{i+1,j}\mathbf{b}_{i+1,j},\\ \mathbf{B}_{i,j} &= a_{i,j}\mathbf{a}_{i,j} + b_{i,j}\mathbf{b}_{i,j}.\end{aligned} \tag{8}$$

Combining (7) and (8), we can obtain a system of linear equations of $\mathbf{b}$ which can be formulated as a single matrix equation:

$$\mathbf{HP} = \mathbf{c}, \tag{9}$$

where $\mathbf{H}$ represents a sparse matrix containing all the coefficients of $\mathbf{b}_{i,j}$. $\mathbf{P}$ is the vector of length $n \times m$ containing all the unknown length values $\mathbf{b}_{i,j}$, and $\mathbf{c}$ is a vector with all zero elements. After setting one surface point to a given value in the column vector $\mathbf{c}$, we can get a unique least-squares solution as:

$$\mathbf{P} = (\mathbf{H}^{\mathrm{T}}\mathbf{H})^{-1}\mathbf{H}^{\mathrm{T}}\mathbf{c}. \tag{10}$$

The above freeform surface construction algorithm is concretely introduced in Refs. [29], [30].

ACKNOWLEDGMENT

Zhengbo Zhu thanks Shili Wei for his valuable help in establishing the integrable ray mapping.

REFERENCES

[1] Z. Ding et al., "Direct design of thin and high-quality direct-lit LED backlight systems," *IEEE Photon. J.*, vol. 13, no. 2, Apr. 2021, Art. no. 8200210.
[2] Z. Zhu et al., "Compact freeform primary lens design based on extended Lambertian sources for liquid crystal display direct-backlight applications," *Opt. Eng.*, vol. 58, no. 2, pp. 025108–025108, 2019.
[3] S. Kikuchi et al., "Thin mini-LED backlight using reflective mirror dots with high luminance uniformity for mobile LCDs," *Opt. Exp.*, vol. 29, no. 17, pp. 26724–26735, 2021.
[4] Q. Feng et al., "Ultrathin miniLED backlight system using optical film with microstructures," *Appl. Opt.*, vol. 60, no. 30, pp. 9497–9503, 2021.
[5] B. Kim et al., "Eliminating hotspots in a multi-chip LED array direct backlight system with optimal patterned reflectors for uniform illuminance and minimal system thickness," *Opt. Exp.*, vol. 18, no. 8, pp. 8595–8604, 2010.
[6] G. W. Yoon et al., "Edge-lit LCD backlight unit for 2D local dimming," *Opt. Exp.*, vol. 26, no. 16, pp. 20802–20812, 2018.
[7] Q. Feng et al., "Secondary optical design for LED backlight luminance improvement of helmet-mounted display," *J. Display Technol.*, vol. 12, no. 6, pp. 577–582, 2016.
[8] K. Sako et al., "50-2: Development of new head-up display system utilizing RGBW LCD and local dimming backlight," *SID Symp. Dig. Tech. Papers*, vol. 47, no. 1, pp. 680–683, 2016.
[9] K. Kamoshida et al., "18-2: Improvement of the light leakage of HUD system," *SID Symp. Dig. Tech. Papers*, vol. 51, no. 1, pp. 250–253, 2020.
[10] D. Z. Lin et al., "Development of a quasi-collimated UV LED backlight for producing uniform and smooth 3D printing objects," *Opt. Exp.*, vol. 30, no. 9, pp. 14759–14769, 2022.
[11] O. Dross et al., "A superior architecture of brightness enhancement for display backlighting," *Nonimaging Opt. Efficient Illumination Syst. III*, vol. 6338, pp. 117–124, 2006.
[12] C. Han et al., "Fabrication of a controllable anti-peeping device with a laminated structure of microlouver and polymer dispersed liquid crystals film," *Liquid Cryst.*, vol. 46, no. 15, pp. 2235–2244, 2019.
[13] Z. Zhu et al., "Freeform illumination optics design for extended LED sources through a localized surface control method," *Opt. Exp.*, vol. 30, no. 7, pp. 11524–11535, 2022.
[14] S. Wei et al., "Compact freeform illumination optics design by deblurring the response of extended sources," *Opt. Lett.*, vol. 46, no. 11, pp. 2770–2773, 2021.
[15] J. Zou et al., "Doubling the optical efficiency of VR systems with a directional backlight and a diffractive deflection film," *Opt. Exp.*, vol. 29, no. 13, pp. 20673–20686, 2021.
[16] P. Krebs et al., "Homogeneous free-form directional backlight for 3D display," *Opt. Commun.*, vol. 397, pp. 112–117, 2017.
[17] R. Wu et al., "Design of freeform illumination optics," *Laser Photon. Rev.*, vol. 12, no. 7, 2018, Art. no. 1700310.
[18] A. M. McCarthy, J. Romero-Vivas, C. O'Hara, N. Rebrova, L. Lewis, and S. P. Hegarty, "LED-based collimating line-light combining freeform and Fresnel optics," *IEEE Photon. J.*, vol. 10, no. 6, Dec. 2018, Art. no. 8201713.
[19] K. Desnijder, P. Hanselaer, and Y. Meuret, "Freeform Fresnel lenses with a low number of discontinuities for tailored illumination applications," *Opt. Exp.*, vol. 28, no. 17, pp. 24489–24500, 2020.
[20] D. T. Giang, T. S. Pham, Q. M. Ngo, V. T. Nguyen, T. Q. Tien, and P. H. Duong, "An alternative approach for high uniformity distribution of indoor lighting LED," *IEEE Photon. J.*, vol. 12, no. 2, Apr. 2020, Art. no. 7100810.
[21] C. M. Tsai and B. X. Wang, "A freeform mirror design of uniform illumination in streetlight from a split light source," *IEEE Photon. J.*, vol. 10, no. 4, Aug. 2018, Art. no. 2201212.
[22] R. Wu et al., "Direct design of aspherical lenses for extended non-Lambertian sources in two-dimensional geometry," *Opt. Lett.*, vol. 40, no. 13, pp. 3037–3040, 2015.
[23] *Illumination Engineering: Design With Nonimaging Optics*. Hoboken, NJ, USA: Wiley, 2012.
[24] Z. Zhu et al., "Freeform illumination optics for 3D targets through a virtual irradiance transport," *Opt. Exp.*, vol. 29, no. 10, pp. 15382–15392, 2021.
[25] S. Wei, Z. Zhu, Z. Fan, and D. Ma, "Least-squares ray mapping method for freeform illumination optics design," *Opt. Exp.*, vol. 28, pp. 3811–3822, 2020.
[26] W. C. Ernest, *Differential Geometry of Three Dimensions*. New York, NY, USA: The Univ. Press, 1927.
[27] S. Sorgato, J. Chaves, H. Thienpont, and F. Duerr, "Design of illumination optics with extended sources based on wavefront tailoring," *Optica*, vol. 6, pp. 966–971, 2019.
[28] J. C. Minano and P. Benitez, "Fermat's principle and conservation of 2D etendue," *Nonimaging Opt. Efficient Illumination Syst.*, vol. 5529, 2004, Art. no. 9.
[29] Z. Feng, B. D. Froese, and R. Liang, "Freeform illumination optics construction following an optimal transport map," *Appl. Opt.*, vol. 55, pp. 4301–4306, 2016.
[30] S. Wei et al., "Multi-surface catadioptric freeform lens design for ultra-efficient off-axis road illumination," *Opt. Exp.*, vol. 27, no. 12, pp. A779–A789, 2019.